Geophysical Research Letters

RESEARCH LETTER
10.1029/2022GL098061

The History of Water in Martian Magmas From Thorium Maps

Benjamin A. Black[1], Michael Manga[2], Lujendra Ojha[1], Marc-Antoine Longpré[3,4], Suniti Karunatillake[5], and Lisa Hlinka[3,4]

[1]Department of Earth and Planetary Sciences, Rutgers University, Piscataway, NJ, USA, [2]Department of Earth and Planetary Sciences, University of California, Berkeley, Berkeley, CA, USA, [3]School of Earth and Environmental Sciences, Queens College, City University of New York, Queens, NY, USA, [4]Earth and Environmental Sciences, The Graduate Center, City University of New York, New York, NY, USA, [5]Department of Geology and Geophysics, Louisiana State University, Baton Rouge, LA, USA

Abstract Water inventories in Martian magmas are poorly constrained. Meteorite-based estimates range widely, from 10^2 to $>10^4$ ppm H_2O, and are likely variably influenced by degassing. Orbital measurements of H primarily reflect water cycled and stored in the regolith. Like water, Th behaves incompatibly during mantle melting, but unlike water Th is not prone to degassing and is relatively immobile during aqueous alteration at low temperature. We employ Th as a proxy for original, mantle-derived H_2O in Martian magmas. We use regional maps of Th from Mars Odyssey to assess variations in magmatic water across major volcanic provinces and through time. We infer that Hesperian and Amazonian magmas had ~100–3,000 ppm H_2O, in the lower range of previous estimates. The implied cumulative outgassing since the Hesperian, equivalent to a global H_2O layer ~1–40 m deep, agrees with Mars' present-day surface and near-surface water inventory and estimates of sequestration and loss rates.

Plain Language Summary Past volcanism on Mars has supplied some of the water that carved ancient river valleys and shaped the chemistry of the Martian near-surface. However, the amount of water carried by Martian magmas is an open question, in part because igneous rocks and meteorites have often lost their original water contents through degassing. The trace element thorium can be used as a proxy for magmatic water, because thorium and water are transferred in similar proportions to magmas during mantle melting, but thorium does not degas. We use regional maps of thorium from the Mars Odyssey spacecraft to track variations in magmatic water through time and across major volcanic provinces.

Key Points:

- Thorium partitions similarly to H_2O during Martian mantle melting but does not degas, and is useful as a proxy for primary magmatic H_2O
- Gamma Ray Spectroscopy maps of thorium distribution are used to track variations in primary magmatic H_2O through Mars' history
- We infer that Hesperian and Amazonian magmas had ~100–3,000 ppm H_2O, implying outgassing of a global H_2O layer ~1–40 m deep

Supporting Information:

Supporting Information may be found in the online version of this article.

Correspondence to:

B. A. Black,
bblack@eps.rutgers.edu

Citation:

Black, B. A., Manga, M., Ojha, L., Longpré, M.-A., Karunatillake, S., & Hlinka, L. (2022). The history of water in Martian magmas from thorium maps. *Geophysical Research Letters*, *49*, e2022GL098061. https://doi.org/10.1029/2022GL098061

Received 26 JAN 2022
Accepted 20 MAY 2022

Author Contributions:

Conceptualization: Benjamin A. Black, Marc-Antoine Longpré, Lisa Hlinka
Data curation: Benjamin A. Black, Michael Manga, Lujendra Ojha, Marc-Antoine Longpré, Suniti Karunatillake, Lisa Hlinka
Formal analysis: Benjamin A. Black, Suniti Karunatillake
Funding acquisition: Benjamin A. Black, Michael Manga
Investigation: Benjamin A. Black, Michael Manga, Lujendra Ojha, Marc-Antoine Longpré

1. Introduction

The concentration of water in Martian magmas is critical to their petrologic evolution (Balta & McSween, 2013; Filiberto & Treiman, 2009; McSween et al., 2001), eruptibility (Black & Manga, 2016), and explosivity (Moitra et al., 2021). Magmatic water has also strongly influenced the evolution of the Martian hydrosphere (Grott et al., 2011; McSween & Harvey, 1993), with water inventory in the zone of exchange between the Martian crust and atmosphere controlled by the balance between volcanism, mineral sequestration, and loss to space (e.g., Carr & Head, 2015; Scheller et al., 2021). Water outgassing from magmas is thought to be the underlying source for surface water inventories ultimately involved in formation of Martian rivers, lakes or proposed Martian oceans (Clifford & Parker, 2001; Perron et al., 2007). Existing constraints on magmatic water inventories from experimental petrology and meteorites span more than an order of magnitude, from <1,000 to 20,000 ppm (0.1–2 wt.%) H_2O (e.g., Filiberto et al., 2016; Filiberto & Treiman, 2009; McCubbin et al., 2010, 2016; McSween et al., 2001). This range in magma H_2O contents corresponds to a range in expected outgassing of global equivalent water depths of ~10^1–10^2 m (McSween & Harvey, 1993). Assuming 10,000 ppm (1 wt.%) H_2O in Martian magmas, Carr and Head (2015) back-calculated from present-day surface and near-surface water inventories to estimate cumulative Hesperian to Amazonian outgassing of ~8 m global equivalent water, with the majority of the present-day water surface and near-surface water inventory carried over from the Noachian.

Médard and Grove (2006) suggested that Noachian magmas might have been water-rich, with progressive dewatering of the mantle through subsequent volcanic degassing. Unlike on Earth, the absence of plate tectonics on Mars prevents rehydration of the mantle. Evolving melting conditions through time (Baratoux et al., 2011) could

Methodology: Benjamin A. Black, Michael Manga, Lujendra Ojha, Suniti Karunatillake
Visualization: Benjamin A. Black, Marc-Antoine Longpré
Writing – original draft: Benjamin A. Black
Writing – review & editing: Benjamin A. Black, Michael Manga, Lujendra Ojha, Marc-Antoine Longpré, Suniti Karunatillake, Lisa Hlinka

modify the initial volatile budgets of Martian magmas, raising the possibility of secular shifts in magmatic volatiles that could link mantle geodynamics to changes in surface environments on long timescales.

Testing these ideas requires an improved understanding of the history of igneous H_2O on Mars. However, constraints on water from Martian meteorites mostly span a limited Amazonian age range, with a few exceptions such as NWA7533 (Humayun et al., 2013) and ALH84001 (Nyquist et al., 2001). Meteorites also represent isolated samples of specific locations, for example, in Tharsis (Lagain et al., 2021), that may not sample regional chemical variations around Mars (Filiberto, 2017; Filiberto et al., 2016). Moreover, degassing during magma ascent and eruption obscures original, mantle-derived volatile concentrations (McSween & Harvey, 1993).

The Gamma Ray Spectrometer (GRS) on the Mars Odyssey spacecraft provides regional-scale distributions of major and trace elements including Si, Cl, K, Fe, H, and Th (Boynton et al., 2007) spanning Martian equatorial to mid-latitudes (±50°). These spectrally derived chemical maps are laterally coarse at $\sim 10^2$ km scale resolution, and are sensitive to decimeter-scale depths (Baratoux et al., 2011; Boynton et al., 2007; Feldman et al., 2002; Taylor et al., 2010), revealing strong, regionally consistent distinctions in measured chemical compositions across Mars. GRS measurements of H yield near-surface water inventories (Boynton et al., 2007; Feldman et al., 2002; Hood et al., 2019), which reflect the shallow cycling of water in the regolith rather than original igneous distributions.

Here, we explore the use of the incompatible element Th as a proxy for the original, undegassed H_2O concentrations imparted to Martian magmas during mantle melting, which we refer to as the primary magmatic H_2O. Trace element proxies for volatiles in magmas are increasingly applied on Earth to constrain volatile concentrations prior to degassing, on the assumption that proxies can be selected for partitioning behavior during melting and crystallization that resembles specific volatile elements, with the crucial difference that they are impervious to degassing (Rosenthal et al., 2015; Saal et al., 2002). Based on similar bulk partition coefficients during melting of Earth's mantle, Th, Nb, and Ba have been used as proxies for CO_2 (Rosenthal et al., 2015; Saal et al., 2002), Ce has been used as a proxy for H_2O (e.g., Dixon et al., 2002), and K and Nd have been proposed as rough proxies for Cl and F respectively (Workman et al., 2006). While initial work focused on mid-ocean ridge basalts, trace element proxies have also been applied to constrain volatiles prior to degassing from ocean island basalts (Workman et al., 2006) and flood basalts (Hernandez Nava et al., 2021). Direct measurements of trace elements such as Nb, Ba, and Ce are largely unavailable for Mars. However, Th represents a possible substitute for Ce as a proxy for H_2O in Martian magmas. Data from Earth demonstrate that while the correlation between H_2O and Ce in mid-ocean ridge basalts is somewhat cleaner, Th also tracks H_2O, and the fit improves after correction for slight differences in the bulk partition coefficients of Th and H_2O (Figure S1 in Supporting Information S1). Use of Th as a proxy for H_2O offers a useful comparison with constraints from meteorites and rovers because Th is not impacted by degassing, GRS data offer a large-scale perspective on Th (Figure 1; Th is one of the best resolved elements in GRS data), and Th is relatively immobile during low-temperature aqueous alteration (Taylor, Stopar, et al., 2006) implying its distribution likely reflects initial igneous compositions.

2. Mineralogy of the Martian Mantle, Partition Coefficients, and Mantle H_2O/Th

To assess the suitability of Th as a proxy for the behavior of H_2O during melting of the Martian mantle, we combine experimental partitioning data with models for Mars' mantle mineralogy. A trace element's bulk partition coefficient (D) describes its equilibrium distribution between the solid and melt (Rollinson & Pease, 2021). The bulk partition coefficient depends on a given trace element's partition coefficients for specific minerals (D_n) and the proportions of those minerals in the rock undergoing melting (X_n):

$$D = D_1X_1 + D_2X_2 + D_3X_3\ldots \quad (1)$$

We compile estimates of mineral-melt partition coefficients for H_2O and Th in Table S1 in Supporting Information S1. Models of the mineralogy of the Martian mantle (Table S1 in Supporting Information S1) have been developed based on equilibrium phase assemblages determined experimentally (Bertka & Fei, 1997) or with thermodynamic algorithms such as MELTS (Ghiorso & Sack, 1995; Sanloup et al., 1999) for assumed bulk mantle compositions (e.g., Taylor, 2013; Wänke & Dreibus, 1994). The mineralogy of the Martian mantle may have evolved through time, as melt extraction depletes clinopyroxene and aluminous phases. In addition to bulk composition and mineralogy, elemental partitioning can depend on oxygen fugacity and individual mineral

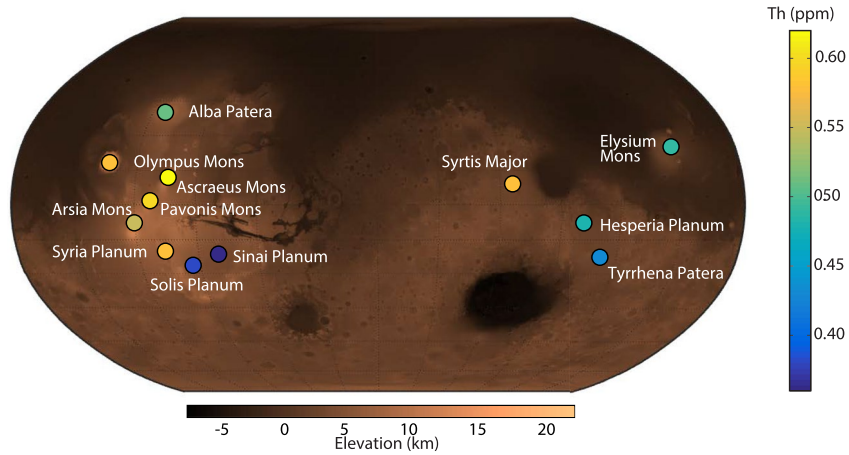

Figure 1. Th concentrations within individual Martian volcanic provinces. Th data (from Baratoux et al., 2011) shown as colored disks overlain on Mars Orbiter Laser Altimeter topography data (Smith et al., 2001).

chemistry (e.g., Dalou et al., 2012; Mysen, 2006). Future experimental data constraining Th and H_2O partitioning under Mars-relevant conditions would further strengthen the approach described here.

The bulk partition coefficients calculated from mantle mineralogy models range from 0.007 to 0.01 for H_2O and 0.001–0.003 for Th; both H_2O and Th are thus highly incompatible, but Th is slightly more so. These slight differences in bulk partition coefficients result in a fractionation during melting that diminishes with increasing melt fraction (Figure 2, Figure S1 in Supporting Information S1). For very small (<3%) degrees of melting, large fractionations in H_2O/Th can result. However, typical melt fractions for Martian magmas are thought to be significantly higher (e.g., 4%–15% from Baratoux et al., 2011; see Table S2 in Supporting Information S1). For this typical range in melt fractions, differences in H_2O and Th bulk partition coefficients result in uncertainties of ~5%–20% assuming modal batch melting (Figure 2). We can correct for this fractionation using estimates of

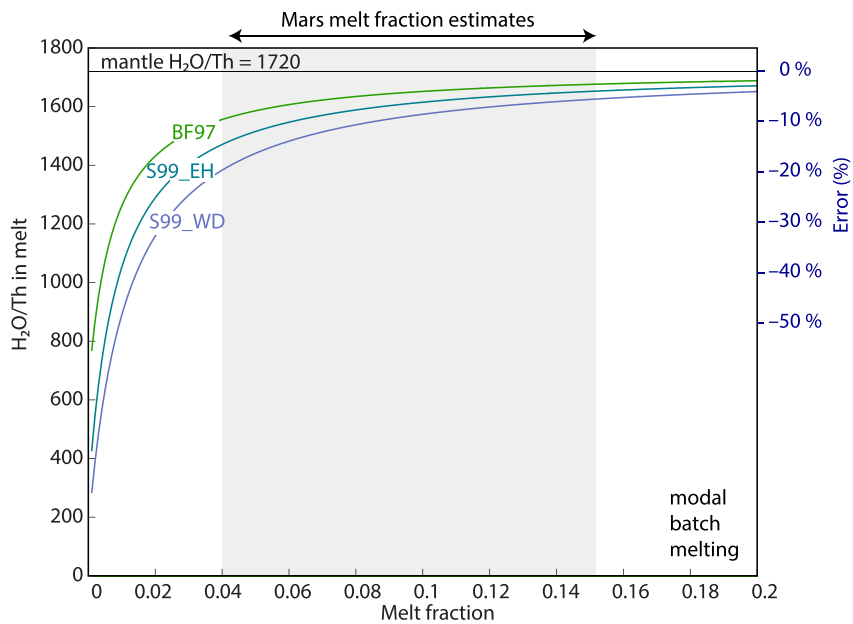

Figure 2. The reliability of Th as a proxy for initial water depends on melt fraction and mantle mineralogy. As melt fraction increases, differences in bulk distribution coefficient between Th and H_2O become less significant. Melt fraction estimates shown are from Baratoux et al. (2011). Depending on assumed mantle mineralogy, for ~4% melting, the errors in calculated melt H_2O introduced due to differences in distribution coefficient are ~10–20%. BF97: Bertka and Fei (1997), S99: Wänke and Dreibus (1994) and H + EH chondrite models from Sanloup et al. (1999). Mantle H_2O/Th = 1,720 is an average of mantle H_2O estimates (i.e., ~96 ppm H_2O) and 0.056 ppm mantle Th.

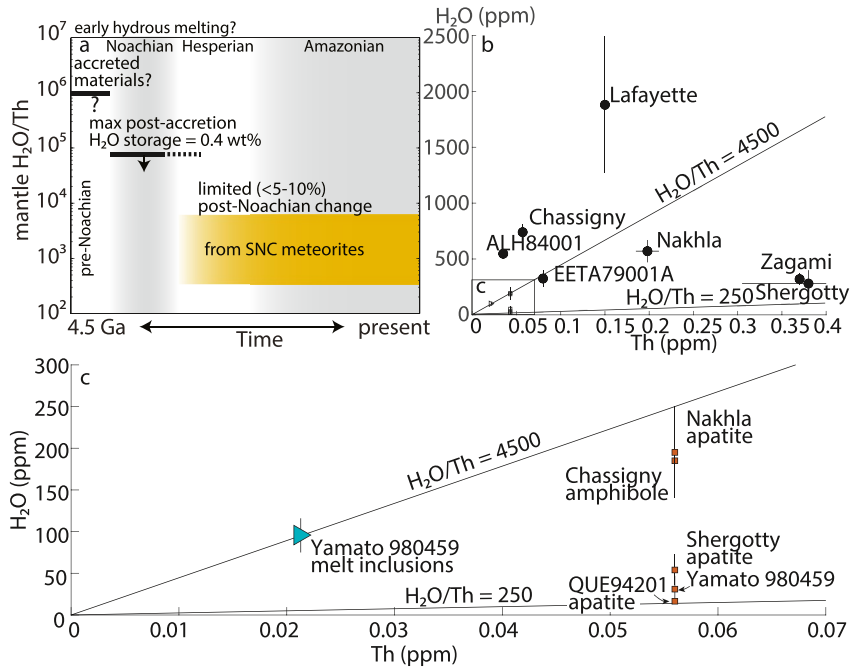

Figure 3. Constraints on mantle H_2O/Th through time and from different lines of evidence. (a) Progressive mantle outgassing and Th depletion due to crust extraction in the first 0.5–1 Gyr (Grott et al., 2011) could cause changes in H_2O/Th, though similar partitioning during melting is expected to limit such changes. Modest (<5%–10%) H_2O outgassing after ~3.5 Ga (Hauck & Phillips, 2002) further suggests stabilization of post-Noachian mantle H_2O/Th. (b) Comparison of Martian meteorite H_2O and Th data with estimated mantle H_2O/Th ratios. Bulk compositions are from Lodders (1998). H_2O data were collected after first heating above 300°C. (c) Enlargement of outlined corner of panel b showing melt inclusion data and selected estimates of mantle H_2O. H_2O data from Yamato 980459 are from olivine-hosted melt inclusions after correction for crystallization (Usui et al., 2012), and bulk Th data for Yamato 980459 are from Shirai and Ebihara (2004). Other mantle H_2O estimates are from Usui et al. (2012), McCubbin et al. (2010, 2012, 2016), Hallis et al. (2012), and Taylor (2013).

degree of melting from Baratoux et al. (2011), who consider two methods: estimation of degree of melting from GRS Th concentrations and the batch melting equation, with assumed mantle Th = 0.056 ppm; and estimation of degree of melting from thermodynamic modeling of melt FeO and SiO_2 compared with GRS observations. The batch modal melting equation relates liquid concentrations for element *i*, $C_{L,i}$, to mantle concentrations, $C_{0,i}$, for a given bulk partition coefficient D and degree of melting F:

$$C_L^i/C_0^i = 1/[D + F(1 - D)] \tag{2}$$

Equation 2 can be re-arranged to calculate F with GRS Th representing Th in the magma, C_L^{Th}:

$$F = \left[C_0^{Th}/C_L^{Th} - D_{Th}\right] / [1 - D_{Th}] \tag{3}$$

Baratoux et al. (2011) found strong agreement between F calculated in this manner and estimates of F from FeO and SiO_2 for Hesperian volcanic provinces. However, a mismatch for some Amazonian volcanic regions including Olympus Mons, Arsia Mons, and Alba Patera suggests the source mantle for these magmas may have been slightly depleted in Th. For these provinces, Baratoux et al. (2011) estimated melt fraction using GRS FeO and SiO_2. We provide estimates of F calculated using Equation 3, and as estimated by Baratoux et al. (2011) in Table S2. For the purposes of subsequent calculations, we adopt values of F from Baratoux et al. (2011). From Equation 2 for melt H_2O and Th, the H_2O/Th ratio in primary, mantle-derived melts is

$$C_L^{H_2O}/C_L^{Th} = C_0^{H_2O}/C_0^{Th} \times [D_{Th} + F(1 - D_{Th})] / \left[D_{H_2O} + F\left(1 - D_{H_2O}\right)\right]. \tag{4}$$

Mantle H_2O/Th ($C_0^{H_2O}/C_0^{Th}$ in Equation 4) represents a major source of uncertainty for inferring absolute abundance (rather than relative variations) in primary H_2O from measured Th concentrations. Constraints on mantle H_2O/Th are summarized in Figure 3. Médard and Grove (2006) estimated ~3.5 wt.% H_2O in bulk accreted material

and envisioned intense hydrous outgassing during accretion. They estimated maximum structurally bound water storage capacity in Mars' mantle of 0.4 wt% H_2O, placing an upper limit on post-accretion mantle water. Constraints on mantle H_2O/Th from igneous clasts within NWA 7034, which contains >4 Ga zircons (Costa et al., 2020), could be critical to constraining the potential evolution of mantle H_2O/Th around this time. Balta and McSween (2013) proposed that Hesperian and Amazonian magmas had generally higher Th and lower H_2O relative to Noachian magmas due to progressive degassing of the mantle. Thermal evolution models have estimated a wide range for the total water lost from the mantle, but generally agree that <5%–15% of the initial water content of the Martian mantle has degassed in the past ~3.5 Ga (Fraeman & Korenaga, 2010; Hauck & Phillips, 2002; Morschhauser et al., 2011; Sandu & Kiefer, 2012). These results imply that mantle H_2O/Th ratios are unlikely to have changed dramatically after an initial phase of accretion-related degassing, that mantle H_2O/Th has been relatively constant since ~3.5 Ga, and that H_2O should be proportional to Th based on similar partitioning during mantle melting.

Estimates of mantle H_2O from Amazonian-age SNC meteorites span a large range, from 14 to 250 ppm (McCubbin et al., 2010, 2012, 2016; Gross et al., 2013; Taylor, 2013; Usui et al., 2012) or perhaps higher (Dudley et al., 2022). For comparison, the mantle source of mid-ocean ridge basalts on Earth contains ~200 ppm H_2O (Le Voyer et al., 2019). The assumptions necessary to backtrack from estimates of magmatic water from meteorites to mantle source H_2O make it challenging to assess how much of the range in estimates of Martian mantle H_2O results from mantle heterogeneity versus methodological uncertainties. For example, estimates of magmatic H_2O based on H_2O concentrations in apatite (Gross et al., 2013; McCubbin et al., 2012, 2016) or amphibole (McCubbin et al., 2010) depend on knowledge of mineral-melt partition coefficients for H_2O. Estimated magmatic H_2O is then corrected to account for crystallization to obtain parental magmatic H_2O (e.g., McCubbin et al., 2012 assume 75%–90% crystallization to reach apatite saturation), and finally a range in melt fraction is assumed to infer mantle source H_2O. Despite uncertainties, meteorite data have been interpreted as evidence for heterogeneities in mantle chemistry. For example, the compilation of McCubbin et al. (2016) includes a depleted shergottite source mantle with 14–23 ppm H_2O, an enriched shergottite source mantle with 36–72 ppm H_2O, and a chassignite source mantle with 140–250 ppm H_2O. Recent work has postulated the enriched shergottite source contains as much as 300–1,000 ppm H_2O (Dudley et al., 2022).

For consistency with melt fraction calculations by Baratoux et al. (2011), we assume mantle Th of 0.056 ppm (Dreibus & Wanke, 1985). Taylor (2013) estimated Th = 0.058 for bulk silicate Mars, which would imply lower mantle Th due to incompatible enrichment of the crust. While mantle heterogeneity (discussed above), melting calculations (Baratoux et al., 2011), and repeated melt extraction from the mantle through geologic time (e.g., Ramsey et al., 2021) imply a range in mantle Th, we expect the H_2O/Th ratio to be relatively constant through time and across mantle domains due to similar partitioning of H_2O and Th during melting.

For a range in source mantle H_2O from 14 to 250 ppm, Martian mantle Th = 0.056 ppm implies mantle H_2O/Th = 250–4,500 during the Hesperian and Amazonian (Figure 3c). We assume this range of H_2O/Th for subsequent calculations, while noting that a slightly lower average mantle Th = 0.043 ppm (accounting for estimates of crust mass and mantle mass, see Supporting Information S1), would imply slightly higher H_2O/Th = 325–5,800. Undegassed glassy melt inclusions from the depleted shergottite Yamato 980459 contain 146–251 ppm H_2O (Usui et al., 2012). Correction for crystallization implies parental magmas with 75–116 ppm H_2O, yielding H_2O/Th ratios overlapping with the upper range of H_2O/Th considered here (Figure 3c). Whole rock H_2O/Th ratios of SNC meteorites (Lodders, 1998) also mostly overlap with H_2O/Th = 250–4,500 (Figure 3b), but must be interpreted with caution because the relationship between bulk H_2O and igneous H_2O is highly uncertain. We therefore choose not to expand the range of H_2O/Th we consider to encompass outliers such as ALH84001, Chassigny, and Lafayette.

3. Do GRS Data Track Regional Bedrock Chemistry?

GRS measurements (including the Th concentrations we use as a proxy for H_2O) represent the column-averaged chemistry of the uppermost decimeters of the Martian regolith. Therefore, whether such measurements reflect the chemistry of global-scale dust redistribution versus local geochemistry represents an important question for efforts to use GRS data to infer igneous compositions (Viviano et al., 2019). Following previous studies, we interpret these data as representative of regional geochemistry based on several lines of evidence. GRS compositions do not fall along a mixing line with estimates of global dust composition (Baratoux et al., 2011). Unlike on Earth where plate tectonics and biologically mediated pedogenesis can accentuate compositional stratification,

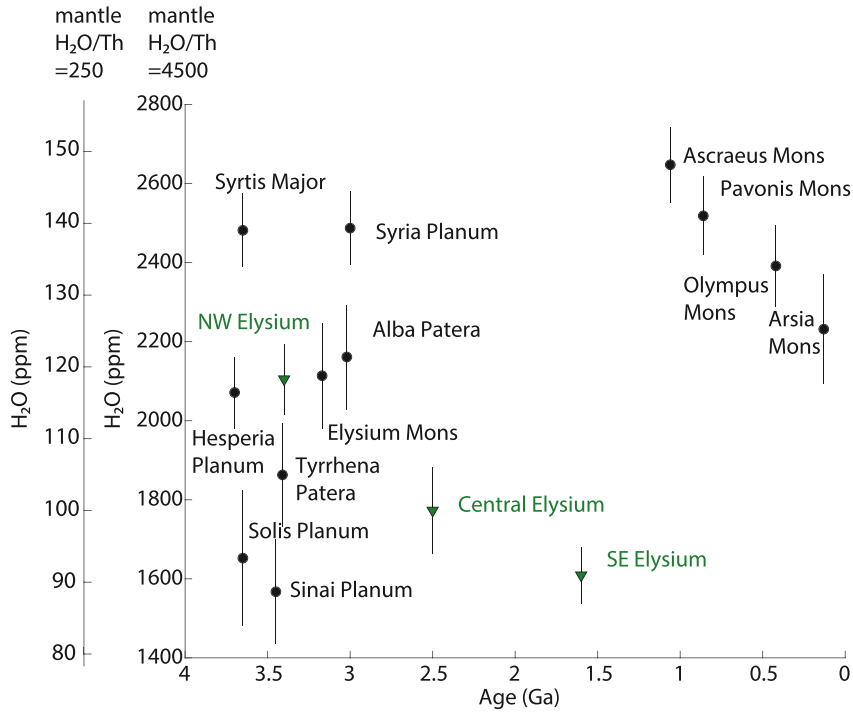

Figure 4. Magmatic H_2O through time from Th data. Variation in inferred primary H_2O in Martian magmas across major volcanic provinces (see Table S2 in Supporting Information S1) for a range in end-member H_2O/Th ratios (dual left axes), after correction for degree of melting as estimated by Baratoux et al. (2011) (Table S2, Equation 4). H_2O estimates from Th data from Baratoux et al. (2011) are shown as circles, with additional estimates from Th data from Elysium sub-provinces (Susko et al., 2017) shown as triangles. Ages and references are given Table S2 in Supporting Information S1. Error bars represent propagated uncertainties from GRS Th data and partition coefficients (see in Supporting Information S1), but do not include uncertainties in H_2O/Th ratio.

Mars' uppermost surface may have undergone extensive homogenization via impact gardening (Taylor, Boynton, et al., 2006). Newsom et al. (2007) focused on GRS data from heavily mantled and less mantled regions based on thermal inertia, albedo, and orbital imagery, and found statistically significant compositional distinctness even among heavily mantled regions such as Arabia, Tharsis, and Acidalia, indicating that these regolith measurements likely reflect variations in underlying bedrock composition. Many of the volcanic regions by Baratoux et al. (2011) considered here, especially those in the southern highlands, show Dust Cover Index values corresponding to only micron-scale dust cover as mapped by Ruff and Christensen (2002).

If regional variations in GRS data reflect processes such as aeolian sorting of fine particles (Viviano et al., 2019) rather than underlying bedrock compositions, then these variations are not meaningful for understanding the evolution of igneous processes. Even in this scenario, mean regolith Th averaged across the full ±50° latitudinal extent of GRS data still constrains the Th concentration in Hesperian and Amazonian crust and by extension the average primary H_2O of Hesperian and Amazonian magmas (Taylor, Boynton, et al., 2006).

4. Constraints on Primary H_2O

For mantle H_2O/Th = 250–4,500, after correcting for slight differences in H_2O and Th partitioning during melting using Equations 3 and 4, the observed range in Th concentrations reported by Baratoux et al. (2011) for Martian volcanic provinces yields estimated primary magmatic H_2O of ~100–3000 ppm (Figure 4). This range falls at the low end of estimates of magmatic H_2O (McSween et al., 2001), but is consistent with recent experimental data (Filiberto & Treiman, 2009), with measurements of H_2O in meteorite apatite and amphibole suggesting ~0.2 wt.% H_2O (McCubbin et al., 2010), and with estimates from sulfur degassing calculations of 0.2–0.4 wt.% H_2O (Gaillard et al., 2013). To some extent agreement with meteorite data is not surprising, because we rely on constraints on mantle H_2O/Th derived from meteorites. However, meteorites represent isolated data points; the

broader GRS dataset supports relatively low primary H_2O for most of the magmas that built Martian volcanic provinces.

GRS data (Figure 4) show substantial variability in Th and implied primary H_2O in the Noachian and Hesperian, progressing to less variability and generally higher Th and higher primary H_2O in the Amazonian. Several factors could contribute to this progression, including secular evolution of bulk mantle H_2O and Th, variations in melting conditions such as changing melt fraction, and heterogeneity in mantle H_2O and Th. We assess each of these factors to interpret data shown in Figure 4.

A range of models have been proposed for the thermal and chemical evolution of the Martian mantle (Fraeman & Korenaga, 2010; Hauck & Phillips, 2002; Morschhauser et al., 2011; Sandu & Kiefer, 2012). However, many of these models agree that mantle evolution was most dramatic in the pre-Noachian and Noachian. For example, Ogawa (2021) proposed a four-stage evolution of the Martian mantle, with a phase of water-rich plume magmatism subsiding into the final stage of thermally driven mantle convection by ~3.5 Ga. Modest magma generation and extraction since the Noachian suggests that H_2O/Th may have remained relatively stable over the past 3.5 Ga. Assuming that GRS data are representative of the same young phases of volcanism in a region that yield the surface ages computed by crater counting (Robbins et al., 2011; Williams et al., 2009), GRS data then provide insights into the evolution of primary H_2O in Martian magmas. Even if H_2O/Th has changed since 3.5 Ga due to repeated melting and mantle degassing, relative differences among volcanic regions of approximately the same age would still be expected to reflect differences in primary H_2O. For example, Alba Patera magmas would be expected to have ~25% more primary H_2O than Tyrrhena Patera magmas (Figure 4).

Hesperian lithospheric thickening (Baratoux et al., 2011), in particular in regions with relatively thin lithosphere in the Noachian, would lead to more uniformly low melt fractions, providing one potential explanation for a progression from variable Th and H_2O to higher Th and H_2O.

Geochemical heterogeneity in the mantle—as documented in meteorites (e.g., Barnes et al., 2020; Moriwaki et al., 2020) and discussed above—could also contribute to variations in magmatic Th and H_2O. The Elysium volcanic province, for which three sub-provinces have been mapped by Susko et al. (2017), provides an opportunity to investigate the temporal evolution in Th and implied H_2O from a plausibly similar mantle source. Th and H_2O concentrations from Elysium (Figure 4) progressively decline for the younger Central and SE Elysium sub-provinces. This temporal evolution contrasts with that of the larger dataset of volcanic provinces from Baratoux et al. (2011). Higher degrees of melting driven by a more vigorous plume or local decreases in lithospheric thickness could explain this pattern within the Elysium province. Alternatively, post-emplacement processes may have modified regional GRS chemistry of the composite volcanic provinces analyzed by Baratoux et al. (2011) more strongly than in the Elysium sub-provinces, where mapped geology and chemical provinces align (Susko et al., 2017). Regardless of the underlying mechanisms, the Elysium data suggest that within individual regions the evolution of magmatic Th and H_2O can encompass far more complexity than is revealed by relatively coarse GRS chemical compositions.

The Martian crust is likely enriched in both Th and H_2O relative to the mantle, including structurally bound H_2O in hydrous mineral phases (Scheller et al., 2021; Wernicke & Jakosky, 2021). Magmatic assimilation or thermal metamorphism of hydrous crustal minerals would increase the flux of H_2O to surface environments.

5. Conclusions and Implications for Outgassing and Eruptive Style

We develop and apply Th as a proxy for primary H_2O concentrations in Martian magmas, and infer typical magmatic water concentrations of 100–3,000 ppm H_2O (Figure 4), with the large range due to uncertainties in mantle H_2O/Th. Similar incompatibility of H_2O and Th suggests that it is conceivable H_2O/Th ratios are relatively constant across enriched and depleted domains in the Martian mantle. As future data (e.g., from meteorites) further constrain mantle H_2O/Th, the Th proxy will provide increasingly accurate estimates of primary H_2O.

We identify an apparent overall decrease in the range of magmatic H_2O from the Noachian to the Amazonian. We recognize possible explanations for this pattern including mantle heterogeneity and conductive thickening of lithospheric thinspots leading to more consistently low degrees of mantle melting. However, we note that Elysium sub-provinces and higher-resolution orbital and rover data demonstrate that when more detailed data are available from individual locations, they can reveal a substantially more complex geochemical evolution.

Crustal production rates from 3.5 Ga to the present have been estimated at $<10^{-1}$–10^{0} km^3/year (Greeley & Schneid, 1991; Morschhauser et al., 2011) with cumulative crustal production of ~570 million km^3 since the Hesperian (Greeley & Schneid, 1991, assuming an intrusive-to-extrusive ratio of 8.5:1). For magmatic water concentrations in the range of 100–3000 ppm H_2O, 100% degassing would deliver 1–40 m of global-equivalent water in the Hesperian and Amazonian (see Supporting Information for details and assumptions). This estimate overlaps with 4–8 m global-equivalent water outgassing in the Hesperian and Amazonian (for 1,000–10,000 ppm H_2O) as estimated by Carr and Head (2015).

Water and chlorine have each been invoked to explain the mineralogy and crystallization temperatures of Martian meteorites (Dann et al., 2001; Filiberto & Treiman, 2009; McSween et al., 2001; Nekvasil et al., 2007). An upper limit on typical primary H_2O concentrations of ~3,000 ppm from our work agrees with the argument, motivated by experimental data and chlorine-rich apatite and amphibole compositions (Filiberto & Treiman, 2009), that chlorine may play an important role in the petrologic evolution of Martian magmas.

Magmatic water concentrations influence whether magmas erupt (Black & Manga, 2016) and the style of eruption (Moitra et al., 2021). Black and Manga (2016) suggested limited concentrations of water and CO_2 in Martian magmas (<15,000 ppm $H_2O + CO_2$) could render them less likely to erupt. In conjunction with low CO_2 concentrations in Martian magmas (Stanley et al., 2011), limited (<3,000 ppm, or 0.3 wt.%) water could thus help to explain relatively high inferred intrusive-to-extrusive ratios on Mars (Black & Manga, 2016). Moitra et al. (2021) describe young (0.05–1 Ma) pyroclastic volcanism in the Cerberus Fossae region, and attribute explosivity to either magmatic or external water. If water concentrations in Martian basalts are typically low, this would favor phreatomagmatic interactions with external water (such as in subsurface icy materials) as a driver of explosive activity.

Data Availability Statement

Underlying data in the form of cumulative gamma photon spectra are available via the PDS: https://pds-geosciences.wustl.edu/missions/odyssey/grs.html) from the Mars Odyssey Gamma Ray Spectrometer suite. GRS Th concentrations for Martian volcanic provinces are given in Table S2 in Supporting Information S1, and are from Baratoux et al. (2011) or in the case of data for Elysium sub-provinces were processed into chemical distributions using published methods (Boynton et al., 2007; Evans et al., 2006; Karunatillake et al., 2007).

Acknowledgments
The authors acknowledge constructive reviews from Kayla Iacovino and an anonymous reviewer. The authors declare no conflicts of interest. BB and MM acknowledge support from NASA Grant 80NSSC19K0545. SK acknowledges support from NASA Grant 80NSSC18K1375.

References

Balta, J. B., & McSween, H. Y., Jr. (2013). Water and the composition of Martian magmas. *Geology*, *41*, 1115–1118. https://doi.org/10.1130/g34714.1

Baratoux, D., Toplis, M. J., Monnereau, M., & Gasnault, O. (2011). Thermal history of Mars inferred from orbital geochemistry of volcanic provinces. *Nature*, *472*, 338–341. https://doi.org/10.1038/nature09903

Barnes, J. J., McCubbin, F. M., Santos, A. R., Day, J. M., Boyce, J. W., Schwenzer, S. P., et al. (2020). Multiple early-formed water reservoirs in the interior of Mars. *Nature Geoscience*, *13*, 260–264. https://doi.org/10.1038/s41561-020-0552-y

Bertka, C. M., & Fei, Y. (1997). Mineralogy of the Martian interior up to core-mantle boundary pressures. *Journal of Geophysical Research*, *102*, 5251–5264. https://doi.org/10.1029/96jb03270

Black, B. A., & Manga, M. (2016). The eruptibility of magmas at Tharsis and Syrtis major on Mars. *Journal of Geophysical Research: Planets*, *120*(9), https://doi.org/10.1002/2016je004998

Boynton, W., Taylor, G., Evans, L. G., Reedy, R., Starr, R., Janes, D., et al. (2007). Concentration of H, Si, Cl, K, Fe, and Th in the low-and mid-latitude regions of Mars. *Journal of Geophysical Research*, *112*. https://doi.org/10.1029/2007JE002887

Carr, M., & Head, J. (2015). Martian surface/near-surface water inventory: Sources, sinks, and changes with time. *Geophysical Research Letters*, *42*, 726–732. https://doi.org/10.1002/2014gl062464

Clifford, S. M., & Parker, T. J. (2001). The evolution of the Martian hydrosphere: Implications for the fate of a primordial ocean and the current state of the northern plains. *Icarus*, *154*, 40–79. https://doi.org/10.1006/icar.2001.6671

Costa, M. M., Jensen, N. K., Bouvier, L. C., Connelly, J. N., Mikouchi, T., Horstwood, M. S. A., et al. (2020). The internal structure and geodynamics of Mars inferred from a 4.2-Gyr zircon record. *Proceedings of the National Academy of Sciences of the United States of America*, *117*, 30973–30979. https://doi.org/10.1073/pnas.2016326117

Dalou, C., Koga, K. T., Shimizu, N., Boulon, J., & Devidal, J. L. (2012). Experimental determination of F and Cl partitioning between lherzolite and basaltic melt. *Contributions to Mineralogy and Petrology*, *163*(4), 591–609. https://doi.org/10.1007/s00410-011-0688-2

Dann, J., Holzheid, A., Grove, T., & McSween, H., Jr. (2001). Phase equilibria of the Shergotty meteorite: Constraints on pre-eruptive water contents of Martian magmas and fractional crystallization under hydrous conditions. *Meteoritics & Planetary Science*, *36*, 793–806. https://doi.org/10.1111/j.1945-5100.2001.tb01917.x

Dixon, J. E., Leist, L., Langmuir, C., & Schilling, J. (2002). Recycled dehydrated lithosphere observed in plume-influenced mid-ocean-ridge basalt. *Nature*, *420*, 385–389. https://doi.org/10.1038/nature01215

Dreibus, G., & Wanke, H. (1985). Mars, a volatile-rich planet. *Meteoritics*, *20*, 367–381.

Dudley, J.-M., Peslier, A. H., & Hervig, R. L. (2022). Shock-induced H loss from pyroxene and maskelynite in a Martian meteorite and the mantle source δD of enriched shergottites. *Geochimica et Cosmochimica Acta*, *317*, 201–217. https://doi.org/10.1016/j.gca.2021.10.020

Evans, L. G., Reedy, R. C., Starr, R. D., Kerry, K. E., & Boynton, W. V. (2006). Analysis of gamma ray spectra measured by Mars Odyssey. *Journal of Geophysical Research*, *111*. https://doi.org/10.1029/2005JE002657

Feldman, W. C., Boynton, W. V., Tokar, R. L., Prettyman, T. H., Gasnault, O., Squyres, S. W., et al. (2002). Global distribution of neutrons from Mars: Results from Mars odyssey. *Science (New York, N.Y.)*., *297*, 75–78. https://doi.org/10.1126/science.1073541

Filiberto, J. (2017). Geochemistry of Martian basalts with constraints on magma Genesis. *Chemical Geology*, *466*, 1–14. https://doi.org/10.1016/j.chemgeo.2017.06.009

Filiberto, J., Baratoux, D., Beaty, D., Breuer, D., Farcy, B. J., Grott, M., et al. (2016). A review of volatiles in the Martian interior. *Meteoritics & Planetary Science*, *51*, 1935–1958. https://doi.org/10.1111/maps.12680

Filiberto, J., & Treiman, A. H. (2009). Martian magmas contained abundant chlorine, but little water. *Geology*, *37*, 1087–1090. https://doi.org/10.1130/g30488a.1

Fraeman, A. A., & Korenaga, J. (2010). The influence of mantle melting on the evolution of Mars. *Icarus*, *210*, 43–57. https://doi.org/10.1016/j.icarus.2010.06.030

Gaillard, F., Michalski, J., Berger, G., McLennan, S. M., & Scaillet, B. (2013). Geochemical reservoirs and timing of sulfur cycling on Mars. *Space Science Reviews*, *174*, 251–300. https://doi.org/10.1007/s11214-012-9947-4

Ghiorso, M. S., & Sack, R. O. (1995). Chemical mass transfer in magmatic processes IV. A revised and internally consistent thermodynamic model for the interpolation and extrapolation of liquid-solid equilibria in magmatic systems at elevated temperatures and pressures. *Contributions to Mineralogy and Petrology*, *119*, 197–212. https://doi.org/10.1007/bf00307281

Greeley, R., & Schneid, B. D. (1991). Magma generation on Mars: Amounts, rates, and comparisons with Earth, moon, and venus. *Science (New York, N.Y.)*, *254*, 996–998. https://doi.org/10.1126/science.254.5034.996

Gross, J., Filiberto, J., & Bell, A. S. (2013). Water in the martian interior: Evidence for terrestrial MORB mantle-like volatile contents from hydroxyl-rich apatite in olivine–phyric shergottite NWA 6234. *Earth and Planetary Science Letters*, *369*, 120–128. https://doi.org/10.1016/j.epsl.2013.03.016

Grott, M., Morschhauser, A., Breuer, D., & Hauber, E. (2011). Volcanic outgassing of CO_2 and H_2O on Mars. *Earth and Planetary Science Letters*, *308*, 391–400. https://doi.org/10.1016/j.epsl.2011.06.014

Hallis, L. J., Taylor, G. J., Nagashima, K., & Huss, G. R. (2012). Magmatic water in the martian meteorite Nakhla. *Earth and Planetary Science Letters*, *359*, 84–92. https://doi.org/10.1016/j.epsl.2012.09.049

Hauck, S. A., & Phillips, R. J. (2002). Thermal and crustal evolution of Mars. *Journal of Geophysical Research*, *107*, 6–1. https://doi.org/10.1029/2001je001801

Hernandez Nava, A., Black, B., Gibson, S., Bodnar, R., Renne, R., & Vanderkluysen, L. (2021). *Reconciling early Deccan Traps CO2 outgassing and pre-KPB global Climate*, *118*(14).

Hood, D., Karunatillake, S., Gasnault, O., Williams, A., Dutrow, B., Ojha, L., et al. (2019). Contrasting regional soil alteration across the topographic dichotomy of Mars. *Geophysical Research Letters*, *46*, 13668–13677. https://doi.org/10.1029/2019gl084483

Humayun, M., Nemchin, A., Zanda, B., Hewins, R., Grange, M., Kennedy, A., et al. (2013). Origin and age of the earliest Martian crust from meteorite NWA [thinsp] 7533. *Nature*, *503*, 513–516. https://doi.org/10.1038/nature12764

Karunatillake, S., Keller, J. M., Squyres, S. W., Boynton, W. V., Brückner, J., Janes, D. M., et al. (2007). Chemical compositions at Mars landing sites subject to Mars Odyssey Gamma Ray Spectrometer constraints. *Journal of Geophysical Research*, *112*. https://doi.org/10.1029/2006JE002859

Lagain, A., Benedix, G., Servis, K., Baratoux, D., Doucet, L., Rajšic, A., et al. (2021). The Tharsis mantle source of depleted shergottites revealed by 90 million impact craters. *Nature Communications*, *12*, 1–9. https://doi.org/10.1038/s41467-021-26648-3

Le Voyer, M., Hauri, E. H., Cottrell, E., Kelley, K. A., Salters, V. J., Langmuir, C. H., et al. (2019). Carbon Fluxes and primary magma CO2 contents along the global mid-ocean ridge System. *Geochemistry, Geophysics, Geosystems*, *20*, 1387–1424. https://doi.org/10.1029/2018gc007630

Lodders, K. (1998). A survey of shergottite, nakhlite and chassigny meteorites whole-rock compositions. *Meteoritics & Planetary Science*, *33*, A183–A190. https://doi.org/10.1111/j.1945-5100.1998.tb01331.x

McCubbin, F. M., Boyce, J. W., Srinivasan, P., Santos, A. R., Elardo, S. M., Filiberto, J., et al. (2016). Heterogeneous distribution of H_2O in the Martian interior: Implications for the abundance of H_2O in depleted and enriched mantle sources. *Meteoritics & Planetary Science*, *51*(11), 2036–2060. https://doi.org/10.1111/maps.12639

McCubbin, F. M., Hauri, E. H., Elardo, S. M., Vander Kaaden, K. E., Wang, J., & Shearer, C. K., Jr. (2012). Hydrous melting of the martian mantle produced both depleted and enriched shergottites. *Geology*, *40*(8), 683–686. https://doi.org/10.1130/g33242.1

McCubbin, F. M., Smirnov, A., Nekvasil, H., Wang, J., Hauri, E., & Lindsley, D. H. (2010). Hydrous magmatism on Mars: A source of water for the surface and subsurface during the Amazonian. *Earth and Planetary Science Letters*, *292*, 132–138. https://doi.org/10.1016/j.epsl.2010.01.028

McSween, H. Y., Grove, T. L., Lentz, R. C., Dann, J. C., Holzheid, A. H., Riciputi, L. R., & Ryan, J. G. (2001). Geochemical evidence for magmatic water within Mars from pyroxenes in the Shergotty meteorite. *Nature*, *409*, 487–490. https://doi.org/10.1038/35054011

McSween, H. Y., Jr., & Harvey, R. P. (1993). Outgassed water on Mars: Constraints from melt inclusions in SNC meteorites. *Science (New York, N.Y.)*, *259*, 1890–1892. https://doi.org/10.1126/science.259.5103.1890

Médard, E., & Grove, T. L. (2006). Early hydrous melting and degassing of the Martian interior. *Journal of Geophysical Research*, *111*.

Moitra, P., Horvath, D. G., & Andrews-Hanna, J. C. (2021). Investigating the roles of magmatic volatiles, ground ice and impact-triggering on a very recent and highly explosive volcanic eruption on Mars. *Earth and Planetary Science Letters*, *567*, 116986. https://doi.org/10.1016/j.epsl.2021.116986

Moriwaki, R., Usui, T., Tobita, M., & Yokoyama, T. (2020). Geochemically heterogeneous Martian mantle inferred from Pb isotope systematics of depleted shergottites. *Geochimica et Cosmochimica Acta*, *274*, 157–171. https://doi.org/10.1016/j.gca.2020.01.014

Morschhauser, A., Grott, M., & Breuer, D. (2011). Crustal recycling, mantle dehydration, and the thermal evolution of Mars. *Icarus*, *212*, 541–558. https://doi.org/10.1016/j.icarus.2010.12.028

Mysen, B. O. (2006). Redox equilibria of iron and silicate melt structure: Implications for olivine/melt element partitioning. *Geochimica et Cosmochimica Acta*, *70*(12), 3121–3138. https://doi.org/10.1016/j.gca.2006.03.014

Nekvasil, H., Filiberto, J., McCubbin, F. M., & Lindsley, D. H. (2007). Alkalic parental magmas for chassignites? *Meteoritics & Planetary Science*, *42*, 979–992. https://doi.org/10.1111/j.1945-5100.2007.tb01145.x

Newsom, H. E., Crumpler, L. S., Reedy, R. C., Petersen, M. T., Newsom, G. C., Evans, L. G., et al. (2007). Geochemistry of Martian soil and bedrock in mantled and less mantled terrains with gamma ray data from Mars Odyssey. *Journal of Geophysical Research*, *112*. https://doi.org/10.1029/2006je002680

Nyquist, L. E., Bogard, D. D., Shih, C. Y., Greshake, A., Stöffler, D., & Eugster, O. (2001). Ages and geologic histories of Martian meteorites. In *Chronology and evolution of Mars* (pp. 105–164). Springer. https://doi.org/10.1007/978-94-017-1035-0_5

Ogawa, M. (2021). The four-stage evolution of Martian mantle inferred from numerical simulation of the magmatism-mantle upwelling feedback. *Journal of Geophysical Research: Planets*, e2021JE006997. https://doi.org/10.1029/2021je006997

Perron, J. T., Mitrovica, J. X., Manga, M., Matsuyama, I., & Richards, M. A. (2007). Evidence for an ancient martian ocean in the topography of deformed shorelines. *Nature*, *447*, 840–843. https://doi.org/10.1038/nature05873

Ramsey, S. R., Howarth, G. H., Udry, A., Gross, J., & Righter, K. (2021). Nickel–manganese variability in olivine and Al-in-olivine thermometry for olivine-phyric shergottites. *Meteoritics & Planetary Science*, *56*(8), 1597–1618. https://doi.org/10.1111/maps.13721

Robbins, S. J., Di Achille, G., & Hynek, B. M. (2011). The volcanic history of Mars: High-resolution crater-based studies of the calderas of 20 volcanoes. *Icarus*, *211*, 1179–1203. https://doi.org/10.1016/j.icarus.2010.11.012

Rollinson, H. R., & Pease, V. (2021). *Using geochemical data: To understand geological processes*. Cambridge University Press.

Rosenthal, A., Hauri, E., & Hirschmann, M. (2015). Experimental determination of C, F, and H partitioning between mantle minerals and carbonated basalt, CO 2/Ba and CO 2/Nb systematics of partial melting, and the CO 2 contents of basaltic source regions. *Earth and Planetary Science Letters*, *412*, 77–87. https://doi.org/10.1016/j.epsl.2014.11.044

Ruff, S. W., & Christensen, P. R. (2002). Bright and dark regions on Mars: Particle size and mineralogical characteristics based on Thermal Emission Spectrometer data. *Journal of Geophysical Research*, *107*(2), 1–222. https://doi.org/10.1029/2001je001580

Saal, A. E., Hauri, E. H., Langmuir, C. H., & Perfit, M. R. (2002). Vapour undersaturation in primitive mid-ocean-ridge basalt and the volatile content of Earth's upper mantle. *Nature*, *419*, 451–455. https://doi.org/10.1038/nature01073

Sandu, C., & Kiefer, W. S. (2012). Degassing history of Mars and the lifespan of its magnetic dynamo. *Geophysical Research Letters*, *39*. https://doi.org/10.1029/2011gl050225

Sanloup, C., Jambon, A., & Gillet, P. (1999). A simple chondritic model of Mars. *Physics of the Earth and Planetary Interiors*, *112*, 43–54. https://doi.org/10.1016/s0031-9201(98)00175-7

Scheller, E. L., Ehlmann, B. L., Hu, R., Adams, D. J., & Yung, Y. L. (2021). Long-term drying of Mars by sequestration of ocean-scale volumes of water in the crust. *Science (New York, N.Y.)*, *372*, 56–62. https://doi.org/10.1126/science.abc7717

Shirai, N., & Ebihara, M. (2004). Chemical characteristics of a martian meteorite, Yamato 980459. *Antarctic Meteorite Research*, *17*, 55. https://doi.org/10.1029/2000je001364

Smith, D. E., Zuber, M. T., Frey, H. V., Garvin, J. B., Head, J. W., Muhleman, D. O., et al. (2001). Mars Orbiter Laser Altimeter: Experiment summary after the first year of global mapping of Mars. *Journal of Geophysical Research*, (1991–2012). *106*, 23689–23722.

Stanley, B. D., Hirschmann, M. M., & Withers, A. C. (2011). CO 2 solubility in Martian basalts and Martian atmospheric evolution. *Geochimica et Cosmochimica Acta*, *75*, 5987–6003. https://doi.org/10.1016/j.gca.2011.07.027

Susko, D., Karunatillake, S., Kodikara, G., Skok, J., Wray, J., Heldmann, J., et al. (2017). A record of igneous evolution in Elysium, a major martian volcanic province. *Scientific Reports*, *7*, 1–11. https://doi.org/10.1038/srep43177

Taylor, G. J. (2013). The bulk composition of Mars. *Geochemistry*, *73*, 401–420. https://doi.org/10.1016/j.chemer.2013.09.006

Taylor, G. J., Boynton, W., Brückner, J., Wänke, H., Dreibus, G., Kerry, K., et al. (2006). Bulk composition and early differentiation of Mars. *Journal of Geophysical Research*, *111*. https://doi.org/10.1029/2005je002645

Taylor, G. J., Martel, L. M., Karunatillake, S., Gasnault, O., & Boynton, W. V. (2010). Mapping Mars geochemically. *Geology*, *38*, 183–186. https://doi.org/10.1130/g30470.1

Taylor, G. J., Stopar, J., Boynton, W. V., Karunatillake, S., Keller, J. M., Brückner, J., et al. (2006). Variations in K/Th on Mars. *Journal of Geophysical Research*, *111*. https://doi.org/10.1029/2006je002676

Usui, T., Alexander, C. M., Wang, J., Simon, J. I., & Jones, J. H. (2012). Origin of water and mantle–crust interactions on Mars inferred from hydrogen isotopes and volatile element abundances of olivine-hosted melt inclusions of primitive shergottites. *Earth and Planetary Science Letters*, *357*, 119–129. https://doi.org/10.1016/j.epsl.2012.09.008

Viviano, C. E., Murchie, S. L., Daubar, I. J., Morgan, M. F., Seelos, F. P., & Plescia, J. B. (2019). Composition of Amazonian volcanic materials in Tharsis and Elysium, Mars, from MRO/CRISM reflectance spectra. *Icarus*, *328*, 274–286. https://doi.org/10.1016/j.icarus.2019.03.001

Wänke, H., & Dreibus, G. (1994). Chemistry and accretion history of Mars. *Philosophical Transactions of the Royal Society of London,Series A: Physical and Engineering Sciences*, *349*, 285–293.

Wernicke, L. J., & Jakosky, B. M. (2021). Martian hydrated minerals: A significant water sink. *Journal of Geophysical Research: Planets*, *126*, e2019JE006351. https://doi.org/10.1029/2019je006351

Williams, D. A., Greeley, R., Fergason, R. L., Kuzmin, R., McCord, T. B., Combe, J., et al. (2009). The circum-Hellas volcanic province, Mars: Overview. *Planetary and Space Science*, *57*, 895–916. https://doi.org/10.1016/j.pss.2008.08.010

Workman, R. K., Hauri, E., Hart, S. R., Wang, J., & Blusztajn, J. (2006). Volatile and trace elements in basaltic glasses from Samoa: Implications for water distribution in the mantle. *Earth and Planetary Science Letters*, *241*, 932–951. https://doi.org/10.1016/j.epsl.2005.10.028

References From the Supporting Information

Baratoux, D., Samuel, H., Michaut, C., Toplis, M. J., Monnereau, M., Wieczorek, M., et al. (2014). Petrological constraints on the density of the Martian crust. *Journal of Geophysical Research: Planets*, *119*, 1707–1727. https://doi.org/10.1002/2014je004642

Broquet, A., & Wieczorek, M. (2019). The gravitational signature of Martian volcanoes. *Journal of Geophysical Research: Planets*, *124*, 2054–2086. https://doi.org/10.1029/2019je005959

Hauri, E. H., Gaetani, G. A., & Green, T. H. (2006). Partitioning of water during melting of the Earth's upper mantle at H 2 O-undersaturated conditions. *Earth and Planetary Science Letters*, *248*, 715–734. https://doi.org/10.1016/j.epsl.2006.06.014

Hiesinger, H., & Head, J., (2004). The Syrtis Major volcanic province, Mars: Synthesis from Mars global surveyor data. *Journal of Geophysical Research*, (1991–2012) *109*(E1). https://doi.org/10.1029/2003je002143

Karunatillake, S., Squyres, S. W., Gasnault, O., Keller, J. M., Janes, D. M., Boynton, W. V., & Finch, M. J. (2011). Recipes for spatial statistics with global datasets: A martian case study. *Journal of Scientific Computing*, *46*, 439–451. https://doi.org/10.1007/s10915-010-9412-z

Knapmeyer-Endrun, B., Panning, M. P., Bissig, F., Joshi, R., Khan, A., Kim, D., et al. (2021). Thickness and structure of the martian crust from InSight seismic data. *Science*, *373*, 438–443. https://doi.org/10.1126/science.abf8966

Lehmann, T., Platz, T., & Michael, G. (2012). *Ages of lava flows in the Hesperia volcanic province*. Lunar and Planetary Science Conference (No. 1659, p. 2526).

Richardson, J. A., Bleacher, J. E., & Glaze, L. S. (2013). The volcanic history of Syria Planum, Mars. *Journal of Volcanology and Geothermal Research*, *252*, 1–13. https://doi.org/10.1016/j.jvolgeores.2012.11.007

Ruj, T., & Kawai, K. (2021). A global investigation of wrinkle ridge formation events; Implications towards the thermal evolution of Mars. *Icarus*, *369*, 114625. https://doi.org/10.1016/j.icarus.2021.114625

Seidelmann, P. K., Archinal, B. A., A'hearn, M. F., Conrad, A., Consolmagno, G., Hestroffer, D., et al. (2007). Report of the IAU/IAG working Group on cartographic coordinates and rotational elements: 2006. *Celestial Mechanics and Dynamical Astronomy*, *98*, 155–180. https://doi.org/10.1007/s10569-007-9072-y

Smrekar, S. E., Lognonné, P., Spohn, T., Banerdt, W. B., Breuer, D., Christensen, U., et al. (2019). Pre-mission InSights on the interior of Mars. *Space Science Reviews*, *215*, 1–72. https://doi.org/10.1007/s11214-018-0563-9

Stähler, S. C., Khan, A., Banerdt, W. B., Lognonné, P., Giardini, D., Ceylan, S., et al. (2021). Seismic detection of the martian core. *Science*, *373*, 443–448.

Wieczorek, M. A., & Zuber, M. T. (2004). Thickness of the Martian crust: Improved constraints from geoid-to-topography ratios. *Journal of Geophysical Research* (1991–2012), 109.

Xiao, L., Huang, J., Christensen, P. R., Greeley, R., Williams, D. A., Zhao, J., & He, Q. (2012). Ancient volcanism and its implication for thermal evolution of Mars. *Earth and Planetary Science Letters*, *323*, 9–18. https://doi.org/10.1016/j.epsl.2012.01.027